

# Solvation structure of coronene-transition metal complex: A RISM-SCF study<sup>†</sup>

Hirofumi Sato,\* Chisa Kikumori, and Shigeyoshi Sakaki

Received Xth XXXXXXXXXXXX 20XX, Accepted Xth XXXXXXXXXXXX 20XX

First published on the web Xth XXXXXXXXXXXX 200X

DOI: 10.1039/b000000x

Coronene (C<sub>24</sub>H<sub>12</sub>) is a flat polyaromatic hydrocarbon consisting of seven peri-fused benzene rings and attracts lots of attention as a fragments of graphene. Using a hybrid method of quantum chemistry and statistical mechanics called RISM-SCF, which is an alternative to QM/MM, the electronic structure and solvation structure of coronene-transition metal complex were computed in a self-consistent manner. The binding of ruthenium complex ([C<sub>5</sub>H<sub>5</sub>Ru]<sup>+</sup>) was extensively studied, especially the changing of the solvation structure.

## 1 Introduction

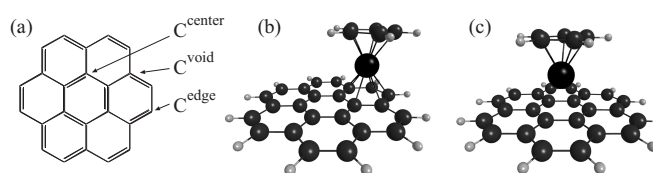
Coronene consists of seven peri-fused benzene rings (Scheme 1), regarded as a small fragment of graphene, which has been attracting increased interest due to its huge potential in electronic applications.<sup>1</sup> A class of carbon-based materials per se is promising. But numerous synthetic studies were also carried out on a novel class of compounds of polycyclic aromatic hydrocarbons (PAHs) with transition metal complex because the functionalisation by transition metal further expands capability of material.

Several interesting characters on the interaction between carbon atoms and metal have become clearer. For example, it is known that the metal is always bonded with two carbon atoms ( $\eta^2$ ) shared between two six membered rings in fullerene (C<sub>60</sub>) but  $\eta^6$ -type coordination, in which the metal is located above the centre of the benzene ring, has never been observed yet. Recently, Alvarez *et al.* reported<sup>2</sup> that  $\eta^6$ -Cp\*Ir complex of 1,2,5,6-tetramethylcorannulene exhibits migration of the Cp\*Ir<sup>2+</sup> unit on the surface of corannulene (C<sub>20</sub>H<sub>10</sub>), which is regarded as a curved-surface fragment of C<sub>60</sub>. On the other hand, several  $\eta^6$ -type coordination complexes have been reported for flat polyaromatic hydrocarbon such as coronene.<sup>3–5</sup> The bonding nature is basically governed by quantum chemistry, but solvation often plays essential role in reality. When a molecule is dissolved into solvent, the electronic structure is affected by the surrounding solvent molecules. It means the electronic structure, which is described by quantum chemistry, and the solvation structure, which is governed by statistical mechanics, are coupled with each other.

We have been developing RISM-SCF<sup>6–9</sup>, which combines

Department of Molecular Engineering, Kyoto University, 615-8510 Japan.  
E-mail: hirofumi@moleng.kyoto-u.ac.jp

two ab initio methods in theoretical chemistry: one is reference interaction site model (RISM)<sup>10,11</sup>, and the other is ab initio molecular orbital (MO) theory. The method determines the electronic structure and solvent distribution around a solute molecule in a self-consistent manner. It is regarded as an alternative to QM/MM method because of the capability to provides information on the electronic structure and microscopic solvation structure. However, one of the remarkable advantages of RISM-SCF is that it enables the use of highly sophisticated quantum chemical method such as CCSD(T) due to the analytical treatment in statistical mechanics<sup>12,13</sup>. RISM-SCF has been successfully applied to numerous molecular phenomena including chemical reactions, chemical equilibria, charge electron processes and so on<sup>14</sup>. In this article, the electronic structure of coronene and its transition-metal complex is considered together with solvation effect. We would like to emphasise that many of the experimental studies have been performed in solution phase, but the effect from solvent, especially on the transition metal is not sufficiently understood. This is because a hybrid type computation such as QM/MM is generally too time-consuming to treat transition metal complex in a reasonably accurate level of theory. Thanks to the analytical nature of the integral equation the-



**Scheme 1:** (a) structure, unique sites and their numbering of coronene. (b)  $\eta^6_{out}$  complex and (c)  $\eta^6_{in}$  complex of [RuCp]<sup>+</sup> and coronene.

ory for molecular liquid, RISM, the electronic structure described in high-level quantum chemical method is obtained together with information of solvation in molecular level. Polarizable continuum model (PCM)<sup>15</sup> is the popular method on electronic structure study of solvation. Since we are focusing also on the changing of the solvation structure, RISM-SCF is preferable in the present study.

## 2 Methods

### 2.1 RISM-SCF Theory

RISM-SCF method compiles *ab initio* electronic structure theory and statistical mechanical theory of molecular liquid. Total energy of solvation system is defined as the sum of quantum chemical energy of the solute ( $E_{\text{solute}}$ ) and solvation free energy ( $\Delta\mu$ )<sup>7</sup>.

$$\mathcal{A} = E_{\text{solute}} + \Delta\mu = \langle \Psi | H_0 | \Psi \rangle + \Delta\mu, \quad (1)$$

Since the electronic structure of the solute molecule and the solvation structure around it are determined in a self-consistent manner, the wave function of the solute molecule is distorted from that in the isolated state. The energy difference between the solute in the isolated state ( $E_{\text{isolated}}$ ) and that in the solution phase ( $E_{\text{solute}}$ ) is a quantity to measure the contribution of solvation effects on the electronic structure.

$$\begin{aligned} E_{\text{reorg}} &= E_{\text{solute}} - E_{\text{isolated}} \\ &= \langle \Psi | H | \Psi \rangle - \langle \Psi_0 | H | \Psi_0 \rangle, \end{aligned} \quad (2)$$

where  $|\Psi\rangle$  and  $|\Psi_0\rangle$  are the wave functions in the solution and in gas phase, respectively. Solvation free energy in the present framework of the theory (excess chemical potential derived under the hyper-netted chain approximation) is given by,

$$\Delta\mu = -\frac{\rho}{\beta} \sum_{\alpha s} \int d\mathbf{r} \left[ c_{\alpha s}(r) - \frac{1}{2} h_{\alpha s}^2(r) + \frac{1}{2} h_{\alpha s}(r) c_{\alpha s}(r) \right], \quad (3)$$

$h_{\alpha s}(r)$  and  $c_{\alpha s}(r)$  are respectively total and direct correlation functions.  $\beta = 1/k_{\text{B}}T$ , where  $k_{\text{B}}$  and  $T$  are the Boltzmann constant and temperature,  $\rho$  is number density of solvent.

Applying variational principle to Eq. (1), the Fock operator of the RISM-SCF theory ( $F^{\text{solv}}$ ) including a solute-solvent interaction,  $V$ , is naturally derived.<sup>7</sup>

$$F^{\text{solv}} = F^{\text{gas}} + V. \quad (4)$$

The interaction energy between the solute and solvent reaction field is given by,

$$\langle \Psi | V | \Psi \rangle = \sum_{\alpha} V_{\alpha} \langle \Psi | b_{\alpha} | \Psi \rangle = \sum_{\alpha} V_{\alpha} q_{\alpha}, \quad (5)$$

**Table 1** Lennard-Jones parameters

	solute			solvent		
	$\sigma^a$	$\epsilon^b$		$\sigma^a$	$\epsilon^b$	$q^c$
C	3.550	0.070	C	3.400	0.109	-0.363
H	2.420	0.030	Cl	3.471	0.265	-0.037
Ru	4.680	0.036	H	2.293	0.016	0.218

The units are respectively <sup>a</sup> Å, <sup>b</sup> kcal mol<sup>-1</sup> and <sup>c</sup> |e|. Note that the electronic structure of the solute is determined in a self-consistent manner.

where  $b_{\alpha}$  is proper population operator for atom  $\alpha$  in the solute molecule and  $V_{\alpha}$  is the electrostatic potential acting on this atom.

$$V_{\alpha} = \rho \sum_s q_s \int \frac{g_{\alpha s}(r)}{r} d\mathbf{r}. \quad (6)$$

Here  $g_{\alpha s}(r) (\equiv h_{\alpha s}(r) - 1)$  is pair correlation function around the solute molecule, namely radial distribution function (RDF). Note that  $V_{\alpha}$  in the present theory is computed based on the microscopic information of solvation structure.

Recently, we developed a new-generation method of RISM-SCF called RISM-SCF-SEDD<sup>9</sup>. In this method, auxiliary basis sets on each atom are prepared to divide electron density into the components assigned on each atom. The great advantage of the procedure is to directly treat spatial electron density distribution (SEDD); it does not require the set of grid points that was necessary to fit to electrostatic potential (ESP) and it is free from these artificial parameter. Furthermore the RISM-SCF-SEDD is quite robust in the computational procedure. The numerical stability significantly expands the versatility of the RISM-SCF family, for example, in treating molecules with buried atoms<sup>16</sup> and transition metals.<sup>17</sup>

### 2.2 Computational Details

The complex formation of  $[\text{CpRu}]^+$  ( $\text{Cp}=\text{C}_5\text{H}_5$ ) to coronene in dichloromethane solvent ( $\text{CH}_2\text{Cl}_2$ ) was considered in the present study. All the computations were performed with density functional theory using GAMESS program package (US version)<sup>18</sup>, which was modified by us to enable the RISM-SCF-SEDD method. B3PW91 functional was chosen as the exchange-correlation term. 6-31G(d) basis set (6d10f) was employed for C and H atoms, and ECP with the corresponding basis set parameters was used for the metal.<sup>19</sup> The gas-phase geometries were adopted to highlight the solvation effect throughout the study.

The RISM integral equation was solved with hyper-netted chain (HNC) closure with the Lennard-Jones parameters listed in Table 1. These for dichloromethane and for the solute C and H are standard ones taken from the literatures.<sup>20</sup> The Ru one was the same as the previous study.<sup>21</sup> The density of

**Table 2** Computed formation energies of [CpRu]<sup>+</sup> complex

	gas phase		dichloromethane	
	$\Delta E_{\text{solute}}$	$\Delta E_{\text{reorg}}$	$\Delta\Delta\mu$	total ( $\Delta\mathcal{A}$ )
$\eta_{\text{out}}^6$	-81.92	-0.39	17.49	-64.82
$\eta_{\text{in}}^6$	-68.40	-0.36	19.82	-48.94

All the values are given in kcal/mol.

dichloromethane was assumed to be 0.009339 molecules/Å. Temperature was taken to be 298.15 K.

### 3 Results

#### 3.1 Energy change on the complex formation

On the complexation of [CpRu]<sup>2+</sup> and coronene, two binding sites were found. One is  $\eta_{\text{out}}^6$ , in which the metal unit binds to a benzene ring of the edge site, and the other is  $\eta_{\text{in}}^6$ , in which the unit is located at the centre of the coronene. In both cases, the Cp-ring is coplanar with the  $\pi$ -surface of coronene with about 2.2 Å of Ru–C distance. Their formation energies are summarised in Table 2. The formation energy in solvent is calculated as the difference between the complex and infinitely separated coronene and [CpRu]<sup>2+</sup>.

$$\Delta\mathcal{A} = \Delta E_{\text{solute}} + \Delta E_{\text{reorg}} + \Delta\Delta\mu, \quad (7)$$

where  $\Delta E_{\text{solute}}$  is the formation energy in gas phase. The relative stability between  $\eta_{\text{out}}^6$  and  $\eta_{\text{in}}^6$  is slightly enhanced in solvent. The result shown in the table suggests that the binding energies are weakened in solvent, but this might come from the well-known overestimation of HNC free energy. Using the gaussian fluctuation (GF) formula  $\Delta\mathcal{A}$ 's are -85.95 kcal/mol ( $\eta_{\text{out}}^6$ ) and -75.11 kcal/mol ( $\eta_{\text{in}}^6$ ), indicating that the binding is strengthened by the solvation. Unfortunately, it is difficult to judge which estimation is closer to the values in the real system, but GF is known to often show better agreement with observations.

The MP2 computations in the gas phase were also performed to estimate the binding energy, showing considerable enhancements; -115.39 kcal/mol ( $\eta_{\text{in}}^6$ ) and -125.13 kcal/mol ( $\eta_{\text{out}}^6$ ). The estimated energy differences between the two isomers are 13.5 kcal/mol (DFT in gas phase), 15.9 kcal/mol (DFT in solution) and 9.7 kcal/mol (MP2 in gas phase). Unfortunately, the MP2 computation in solvent is infeasible but, based on these results, it is very likely that the energy difference is similar to the gas phase one. Anyway, the salient point is that [CpRu]<sup>2+</sup> is  $\eta^6$ -bounded to coronene in the edge position ( $\eta_{\text{out}}^6$ ), consistent with experimental report.<sup>3</sup>

The edge-preference may be simply understood in terms of charge distribution in  $\pi$ -system of coronene. Indeed, the edge-carbon atom (C<sup>edge</sup>) is negatively charged compared to the

**Table 3** Mulliken charge ( $|e|$ ) in gas phase and in dichloromethane.

	[CpRu] <sup>+</sup> , C <sub>24</sub> H <sub>12</sub> <sup>a</sup>		$\eta_{\text{in}}^6$		$\eta_{\text{out}}^6$	
	$q^{\text{gas}}$	$\Delta q$	$q^{\text{gas}}$	$\Delta q$	$q^{\text{gas}}$	$\Delta q$
Ru	0.521	0.036	0.013	-0.006	-0.044	-0.008
Cp	0.479	-0.036	0.335	0.018	0.320	0.018
C <sup>centre</sup>	0.007	-0.003	-0.001	-0.003	0.009	-0.002
C <sup>void</sup>	0.123	-0.006	0.155	-0.004	0.127	-0.004
C <sup>edge</sup>	-0.230	-0.006	-0.226	-0.003	-0.214	-0.004
H	0.165	0.011	0.204	0.006	0.206	0.006

<sup>a</sup> The numbers above and below the line are [CpRu]<sup>+</sup> and coronene moiety, respectively.

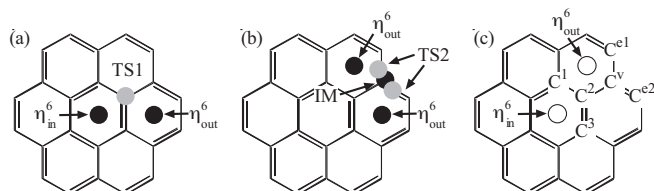
$q^{\text{gas}}$ : Mulliken charge in gas phase.  $\Delta q$ : the difference of Mulliken charge in dichloromethane from the gas phase value. The averaged values of the equivalent atoms are listed for the C<sub>24</sub>H<sub>12</sub> moiety.

central ones (Table 3). The edge-hydrogen atoms also show noticeable change on the formation. Interestingly the changes in C<sup>void</sup> are considerable compared to the directly bonding C<sup>centre</sup> on the complexation of  $\eta_{\text{in}}^6$ . On the other hand, the change in  $\eta_{\text{out}}^6$  formation does not look so significant partly due to a simple averaging over all the atoms in different situations. The solvation effect in electronic structure is moderate except for the isolated [CpRu]<sup>+</sup>, in which all the atoms are exposed to solvent. Presumably, the changing in electronic structure on the formation is neutralised by the  $\pi$ -system. This is a reason why the energy difference between  $\eta_{\text{out}}^6$  and  $\eta_{\text{in}}^6$  in dichloromethane is essentially unchanged from the gas phase value (Table 2).

The scheme of orbital interaction is another important viewpoint. As well known, both of donation (charge transfer from HOMO of PAH to the metal  $d$ -orbital) and back-donation (from the metal to LUMO of PAH) could occur between the metal and  $\pi$ -conjugated system, and the former is dominative in the preset complex. The amplitude of coronene HOMO is localised at its edge-side, whose phase is matching with the metal's  $d$ -orbital (LUMO).

#### 3.2 Migration of the Ru moiety on the coronene surface

It would be interesting to compare the planarity with the curved surface by seeing whether or not the migration occurs on the planar surface of coronene. Scheme 2 indicates the positions of [CpRu]<sup>+</sup> moiety on the surface corresponding to three local minima and two saddle points computed with DFT. All these points were checked through vibrational frequency calculations and two transition states (TSs) were confirmed, namely TS1 and TS2. The former is related to an isomerisation (a) from  $\eta_{\text{in}}^6$  to  $\eta_{\text{out}}^6$ , and the latter is located on the migration (displacement) path (b) between two different  $\eta_{\text{out}}^6$ . An intermediate (IM) was found on the path. Table 4 lists the computed energy of these structures together with MP2 com-



**Scheme 2:** (a) isomerisation from  $\eta_{in}^6$  to  $\eta_{out}^6$  (b) displacement between  $\eta_{out}^6$ 's. The gray circles correspond to transition state (TS1 and TS2), while the black ones are stable structures including intermediate (IM). (c) The labeling to specify the geometry. See Table 5.

putations.

The barrier height of the isomerisation path from  $\eta_{in}^6$  to  $\eta_{out}^6$  through TS1 is computed as 26.7 kcal/mol (DFT) and 40.1 kcal/mol (MP2) in gas phase. In dichloromethane solvent, the barrier height is slightly decreased to 25.6 kcal/mol (DFT). Because of the great binding energy (Table 2), the value of TS1 energy is still lower than the reactant, namely separated coronene and  $[CpRu]^+$ . At all events,  $\eta_{in}^6$  is considered to gradually isomerise to  $\eta_{out}^6$ . Note that the  $[CpRu]^+$  moiety does not cross over the C–C bond via  $\eta^2$ -coordination, instead,  $\eta^1$ -bound with C<sup>centre</sup> is the structure of TS1.

On the displacement path, an intermediate was found, in which the Ru moiety is located just above one of C<sup>edge</sup> in the vicinity of TS (TS2). The computed activation barriers are higher than those in the curved surface, corannulene complex. The barrier obtained by DFT is more than 30 kcal/mol, and even higher by MP2 estimation. As seen in the table, the computed energies of IM and TS2 are very close each other, though MP2 energy of IM is slightly higher that of TS2. We can not rule out the possibility that IM is an artifact in the DFT computation, which might be replaced with TS. It should be stressed that both of TS and IM are too high in energy to migrate through these structures in reality. The population analysis shows that the donation to the metal is relatively weak near the TSs compared to the corannulene case, which may be the reason of the high barrier in the present coronene system.

**Table 4** Energy change on the migration of Ru moiety<sup>a</sup>

	$\eta_{in}^6$	TS1	IM	TS2
DFT (gas)	13.52	40.21	33.48	33.65
$\tilde{\nu}_{im}^b / \text{cm}^{-1}$	—	(90.6i)	—	(67.8i)
DFT (sol)	15.88	41.45	31.19	31.23
MP2 (gas)	9.74	49.83	51.22	51.01

<sup>a</sup> Relative energies with respect to  $\eta_{out}^6$  given in kcal mol<sup>-1</sup>. Total energies of  $\eta_{out}^6$  are -1208.80070 E<sub>h</sub> (DFT) and -1205.38496 E<sub>h</sub> (MP2). <sup>b</sup> Imaginary frequencies obtained by the DFT computations.

A set of selected bond distances between Ru and carbon

**Table 5** Distance between Ru and carbon atoms (Å) at optimized geometries. See Scheme 2(c).

	$\eta_{out}^6$	$\eta_{in}^6$	TS1	IM	TS2
C <sup>1</sup> –Ru	2.32	2.33	2.70	3.66	3.70
C <sup>2</sup> –Ru	2.32	2.33	2.24	2.91	2.89
C <sup>3</sup> –Ru	3.42	2.33	2.57	3.65	3.54
C <sup>v</sup> –Ru	2.31	3.41	2.62	2.21	2.23
C <sup>e1</sup> –Ru	2.23	4.19	3.39	2.43	2.54
C <sup>e2</sup> –Ru	3.40	4.19	3.26	2.42	2.37

The shortest bonds are indicated with italics.

atoms at the critical geometries are listed in Table 5. Though the symmetry is slightly broken because of the Cp ring, the shortest bond listed in the table clearly characterises the structure of each state. The Ru moiety in  $\eta_{out}^6$  and  $\eta_{in}^6$  are positioned at the centre of the benzene ring; all the C<sup>centre</sup>–Ru bonds are equivalent in  $\eta_{in}^6$  while the moiety is slightly shifted from the centre outward in  $\eta_{out}^6$  (C<sup>edge</sup>–Ru is the shorter than C<sup>centre</sup>–Ru). As mentioned above, IM and TS2 are very close each other in energy but their geometries are evidently different. The energy surface in this region is considered to be flat.

### 3.3 Solvation structure

Solvation structure is described based on a probability to find solvent molecule in the vicinity of solute molecule. In the RISM-SCF, radial distribution function (RDF) represents a microscopic character of solvation.

**3.3.1 Coronene and Ru complex** Figure 1 shows RDFs of coronene in dichloromethane solvent (CH<sub>2</sub>Cl<sub>2</sub>) computed by RISM-SCF-SEDD method. The solvation is relatively mild and the distribution of solvent molecule is simply determined by the contact of molecule. The edge carbon (b) shows a little structure around 4Å, probably being related to small interaction between edge-hydrogen and Cl of solvent, which makes a small peak in the Cl–H RDF (not shown). All the

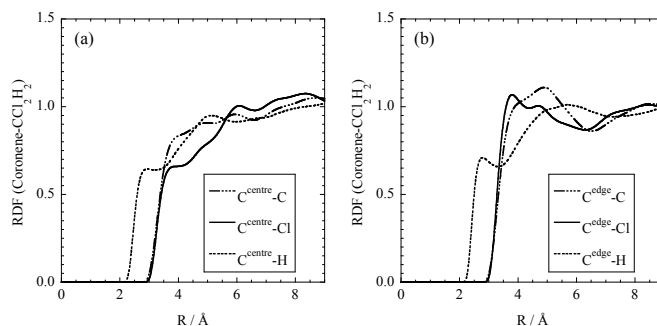


**Fig. 1** RDFs between coronene and dichloromethane solvent. (a) the central carbon atom (C<sup>centre</sup>) and (b) the edge carbon (C<sup>edge</sup>).

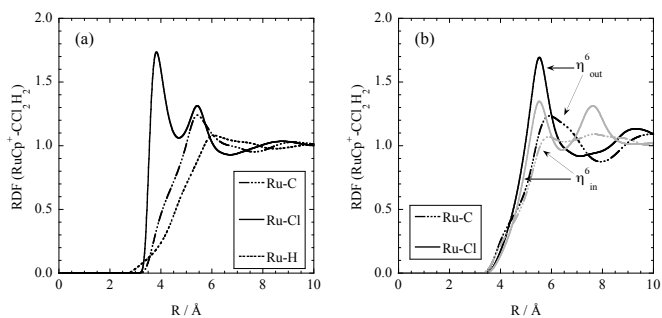


**Fig. 2** RDFs between Ru moiety and dichloromethane solvent. (a) the isolated  $[\text{RuCp}]^+$  and (b) the moiety in the complex of  $\eta_{\text{out}}^6$  and  $\eta_{\text{in}}^6$ .

RDFs quickly approach to the bulk density (one in the vertical axis), indicating that there is no specific interaction between coronene and solvent. But the electronic structure of the coronene is slightly polarized on the solvation. For example, because of the interaction with Cl mentioned above, Mulliken population on the hydrogen atom is changed as shown in Table 3.

Figure 2 is RDF around Ru of  $[\text{RuCp}]^+$ . Because of its positive charge,  $[\text{RuCp}]^+$  attracts solvent molecule, especially Cl atom, and a distinct peak appears around  $4.0\text{\AA}$ . The peak corresponds to a direct contact of Ru and Cl according to their radius,  $(4.68 + 3.47)/2 = 4.08\text{\AA}$  (see Table 1). Due to the delocalisation of positive charge over the complex, Ru and Cp ring share evenly the excess positive charge. As mentioned above, solvation slightly enhances the positive charge on Ru, probably caused by the specific solvation of Cl site. It should be noted, however, that the peak height is rather low, less than 2. The number of solvating Cl atom is estimated to be 3.3 by integration up to the minimum beyond the first peak ( $4.7\text{\AA}$ ). Unfortunately, the enormously broad and obscure first peak of Ru-C RDF makes it difficult to directly estimate the coordination number of solvent molecule.

Figure 2 (b) illustrates the RDFs of Ru moiety in  $\eta_{\text{out}}^6$  and  $\eta_{\text{in}}^6$  complex. The rising of RDF gets moderate and the peak-top is distinctly shifted backward. This is caused by the exclusion of directly attaching solvent molecules on the complexation. Resultingly, Ru atom is sandwiched by Cp and coronene, hence the solvent is allowed to access to the Ru only through the interspace between the  $\pi$ -surfaces. Compared to  $\eta_{\text{in}}^6$ , Ru moiety in  $\eta_{\text{out}}^6$  exposes to the solvent, and more accessible. Hence the RDF of  $\eta_{\text{out}}^6$  is higher than that of  $\eta_{\text{in}}^6$ .

**3.3.2 RDF change in the complexation of  $\eta_{\text{out}}^6$  and  $\eta_{\text{in}}^6$**   
 Finally, the RDF changes on the complexation are depicted in Figure 3. Because of the highly symmetric nature of coronene, the changing is simply classified into three groups, namely, the centre, void and edge carbons. Because the  $[\text{RuCp}]^+$  moiety is bounded with the centre carbons in  $\eta_{\text{in}}^6$ , their RDFs re-

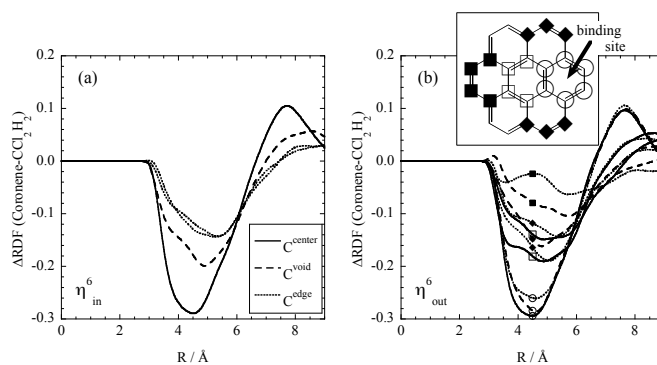


**Fig. 3** Change of RDF with carbon(dichloromethane) on the complexation of (a)  $\eta_{\text{in}}^6$  and (b)  $\eta_{\text{out}}^6$ ;  $\text{C}^{\text{centre}}$  (solid),  $\text{C}^{\text{void}}$  (dashed-dotted) and  $\text{C}^{\text{edge}}$  (dotted). The positions in  $\eta_{\text{out}}^6$  (right-hand side) are indicated with the marks; for example,  $\circ$  corresponding to the binding site.

ceives the greatest changing, namely the solvent molecules are kicked out on the complexation. The considerable decreasing found around  $4.5\text{\AA}$  is evidently related to the directly solvating dichloromethane molecule. The neighbouring void carbon atoms get the next biggest change. The essential trend is very similar in the case of  $\eta_{\text{out}}^6$ . The binding sites indicated with open circle are considerably affected, and the solvent molecule are crowded out by Ru moiety. The number of the solvent pushed away on the complexation may be evaluated by integrating over the negatively value area, e. g., from  $2.9\text{\AA}$  to  $6.7\text{\AA}$  for  $\text{C}^{\text{centre}}$ , which is about 1.6. It suggests that a few number of solvent molecules, which occupies the surface of coronene, is replaced with Ru moiety on the complexation.

According to the RDFs shown above, the interaction between the solute (coronene,  $[\text{RuCp}]^+$  and their complex) and solvent is essentially governed by a simple excluded volume effect, and the solvation is readily replaced with the Ru moiety on the binding. Additionally, the effect from the solvent without specific interaction such as hydrogen bonding does not strongly change the electronic structure of the solute.

## 4 Conclusions

In this contribution, the solvation structure and electronic structure of coronene - transition metal complex were reported using a hybrid method of quantum chemistry and statistical mechanics for molecular liquid called RISM-SCF-SEDD. The solvation effect modifies the electronic structure of solute molecule, and, at the same time, this modification affects the structure of the solvent molecules surrounding the solute. The present methods enables us to evaluate the relative stability of isomers and the possibility of the migration among them.

Because of the relatively mild solvation effect of

dichloromethane, the relative energy among the isomers is almost unchanged upon the solvation. In reality, it is likely that both of  $\eta_{\text{in}}^6$  and  $\eta_{\text{out}}^6$  are formed very quickly, but the latter is greatly stable.  $\eta_{\text{in}}^6$  is then gradually isomerised into  $\eta_{\text{out}}^6$  via the barrier with about 27 kcal/mol.

## Acknowledgments

This work has been financially supported by the Grant-in Aids (19350010, 20550013, 452-20031014 and 461), all supported by the Ministry of Education, Culture, Sports, Science and Technology (MEXT) Japan. We acknowledge Marvin Jose Fernandez for his careful reading of manuscript.

## References

- 1 J. Wu, W. Pisula, K. Müllen, *Chem. Rev.*, **107**, 718 (2007).
- 2 C. M. Alvarez, R. J. Angelici, A. Sygula, R. Sygula, and P. W. Rabideau, *Organometallics*, **22**, 624 (2003).
- 3 T. Jon Seiders, K. K. Baldrige, J. M. O'Connor and J. S. Siegel, *J. Am. Chem. Soc.*, **119**, 4781 (1997).
- 4 M. W. Stoddart, J. H. Brownie, M. C. Baird, H. L. Schmider, *J. Organometallic Chem.*, **690**, 3440 (2005).
- 5 I. Chávez, A. Cisternas, M. Otero, E. Román, *Z. Naturforsch.*, **45b**, 658 (1990).
- 6 S. Ten-no, F. Hirata, and S. Kato, *Chem. Phys. Lett.*, **225**, 202 (1994).
- 7 H. Sato, F. Hirata, and S. Kato, *J. Chem. Phys.*, **105**, 1546 (1996).
- 8 H. Sato, A. Kovalenko and F. Hirata, *J. Chem. Phys.*, **112**, 9463 (2000).
- 9 D. Yokogawa, H. Sato and S. Sakaki, *J. Chem. Phys.*, **126**, 244054 (2007).
- 10 D. Chandler, H. C. Andersen, *J. Chem. Phys.*, **57**, 1930 (1972).
- 11 F. Hirata, P. J. Rossky, *Chem. Phys. Lett.*, **83**, 329 (1981).
- 12 K. Iida, D. Yokogawa, A. Ikeda, H. Sato and S. Sakaki *Phys. Chem. Chem. Phys.*, **11**, 8556 (2010).
- 13 S. Hayaki, K. Kido, H. Sato and S. Sakaki *Phys. Chem. Chem. Phys.*, **12**, 1822 (2010).
- 14 *Molecular Theory of Solvation*, edited by F. Hirata, Kluwer Academic Publishers, Dordrecht Hardbound, 2003.
- 15 J. Tomasi, B. Mennucci, R. Cammi *Chem. Rev.*, **105**, 2999 (2005).
- 16 K. Iida, D. Yokogawa, H. Sato and S. Sakaki *Chem. Phys. Lett.*, **443**, 264 (2007).
- 17 S. Hayaki, D. Yokogawa, H. Sato and S. Sakaki *Chem. Phys. Lett.*, **458**, 329-332 (2008).
- 18 M. W. Schmidt, K. K. Baldrige, J. A. Boatz, S. T. Elbert, M. S. Gordon, J. H. Jensen, S. Koseki, N. Matsunaga, K. A. Nguyen, S. J. Su, T. L. Windus, M. Dupuis, J. A. Montgomery *J. Comput. Chem.*, **14**, 1347 (1993).
- 19 A. W. Ehlers, M. Böhme, S. Dapprich, A. Gobbi, A. Höllwarth, V. Jonas, K. F. Köhler, R. Stegmann, A. Veldkamp, G. Frenking, *Chem. Phys. Lett.*, **208**, 111 (1993); M. Couty, M. B. Hall, *J. Comp. Chem.*, **17**, 1359 (1996).
- 20 T. Fox and P. A. Kollman, *J. Phys. Chem. B*, **102**, 8070 (1998); W. D. Cornell, P. Cieplak, C. I. Bayly, I. R. Gould, K. M. Merz, Jr., D. M. Ferguson, D. C. Spellmeyer, T. Fox, J. W. Caldwell and P. A. Kollman, *J. Am. Chem. Soc.*, **117**, 5179 (1995).
- 21 H. Sato and F. Hirata, *J. Phys. Chem. A*, **106**, 2300 (2002); H. Sato, I. Kawamoto, D. Yokogawa and S. Sakaki, *J. Mol. Liq.*, **136**, 194 (2007).